JOURNAL OF CATALYSIS 110, 191–196 (1988)

NOTES

A Study of Small Pt Particles on Amorphous Al_2O_3 and α-Al_2O_3{0001} Substrates Using TPD of CO and H_2[1]

INTRODUCTION

Recent studies have demonstrated that single crystals exhibit reactivities which are very similar to those observed on real supported catalysts and that reactions which depend on particle size also depend on crystal plane (*1–3*). Since adsorption properties can also be affected by crystal plane, we have recently undertaken a temperature-programmed desorption (TPD) study on small supported particles of varying size to determine if similarities also exist in this property. We have used TPD for examining adsorption since desorption peak temperatures are a sensitive measure of the adsorption bond. We chose to examine Pt because the desorption temperatures for many adsorbates vary dramatically with crystal plane (*4, 5*), unlike other metals like Pd and Rh (*6*). Studies were carried out on samples prepared on flat substrates in order to avoid the complications which arise in TPD due to readsorption and diffusion on porous materials (*7–10*).

In previous studies of CO desorption from Pt particles on amorphous alumina, we have shown that the TPD curves are strongly dependent on particle size (*11*). For very small particles, a single desorption state was observed with a peak temperature at 510 K, the same temperature observed for highly stepped Pt crystals (*12, 13*). For larger particles, we observed a second desorption feature centered at 400 K, which we associated with (111) terraces since this is the peak temperature found for Pt(111) crystals (*14*). This peak at 400 K grew continuously with particle size relative to the peak at 510 K, implying that adsorption of CO on small Pt particles is similar to adsorption on bulk metals and that particle size affects the structure of the sites found on the particles.

In this paper, we have addressed the following questions: (1) What effect does the structure of support have on the Pt particles and their adsorption properties, and (2) can the trends observed with CO adsorption be observed with other simple gases? By comparing TPD curves for CO on small Pt particles on amorphous alumina and on an α-Al_2O_3{0001} crystal, we have demonstrated that desorption of CO from a Pt particle of a given size appears to be independent of the structure of the alumina support, implying that the support structure does not directly affect the metal. By studying TPD of H_2 on Pt particles, we have found that the trend of peak temperatures increasing with decreasing particle size found with CO is *not* observed with H_2, even though stepped crystals of H_2 also exhibit high-temperature states (*15*). From this, we conclude that the sites on these particles should probably not be viewed as extended crystal planes.

The equipment and procedures used in these experiments have been described previously (*11*). The samples could be rotated in front of an Ar^+ ion gun for cleaning, a Pt source for depositing metal overlayers, or an Auger electron spectrometer (AES). A quartz–crystal, film thickness monitor was positioned in front of the Pt source in order to measure the metal flux to the substrate. All experiments were carried out at pressures in the 10^{-10}-Torr range, and clean Pt

[1] This work has been supported by the DOE, Basic Energy Sciences, under Grant DE-FG02-ER 13350. Some facilities were provided by the NSF, MRL Program, under Grant DMR 82-16718.

0021-9517/88 $3.00
Copyright © 1988 by Academic Press, Inc.
All rights of reproduction in any form reserved.

films could be deposited without need for further treatment. The amorphous alumina substrate was prepared by depositing a 500-nm, Al film onto a Ta foil, followed by heating the Al in 1×10^{-8} Torr of O_2 at 800 K until AES showed only a single peak near 51 eV which is indicative of oxidized Al. The crystalline substrate was a $15 \times 7 \times 0.5$-mm wafer, oriented in the {0001} direction. A 300-nm gold film was evaporated onto the back of the crystal, and two Ta wires were clamped onto the crystal with insulating ceramic posts. The sample was heated resistively by passing current through the Ta leads; a Chromel–Alumel thermocouple pressed against the back of the crystal with one of the ceramic posts was used to monitor the temperature.

RESULTS AND DISCUSSION

Growth of the Pt Film

To characterize the growth of the metal films, we monitored the Pt(238-eV) and the O(503-eV) Auger peaks as a function of metal exposure at 300 K, as shown in Fig. 1a. The peak heights in this figure have been normalized to that of bulk Pt and bulk alumina, respectively. The data points shown are for the sapphire crystal. The results for Pt deposition on amorphous alumina have been published previously and are summarized by the solid line, while the calculated peak heights for layer-by-layer growth using an electron mean free path of 0.71 nm are given in the dashed line. (The value of 0.71 nm for the mean free path was calculated from the attenuation of the O(503-eV) peak at the first break point for the amorphous sample and is within the range of 0.6–0.9 nm expected for 500-eV electrons escaping from a solid (*16, 17*). At 300 K, the Pt(238-eV) peak height increases much more slowly and the O(503-eV) peak is attenuated much more slowly with Pt coverage on the crystal than on the amorphous alumina. In addition, the peak heights on sapphire do not vary linearly with the Pt coverage. These observations indicate that the Pt atoms have sufficient mobility on the crystalline surface at 300 K to form three-dimensional (3-D) particles, while the metal overlayers grow in a layer-by-layer manner at this temperature on the amorphous sample.

Further evidence that 3-D particles are

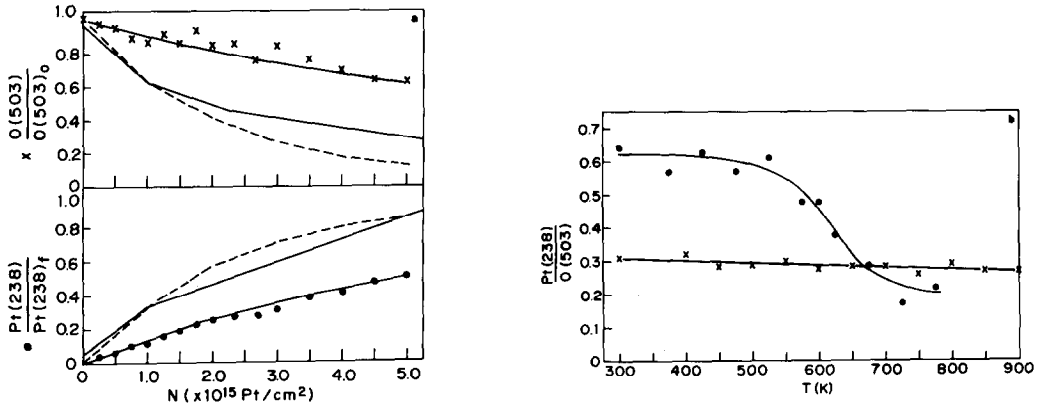

FIG. 1. (a) AES intensities for the Pt(238-eV) and O(503-eV) peaks plotted as a function of metal exposure at 300 K. The peak heights have been normalized to the intensities obtained for bulk Pt and alumina. Data points are shown only for the α-Al_2O_3{0001} sample. Results for the amorphous alumina are represented by the solid lines, while the dashed lines are calculated intensities assuming layer-by-layer growth with an electron mean free path of 0.71 nm. (b) Plot of the Pt(238-eV)/O(503-eV) peak ratio as a function of temperature for a Pt coverage of 2×10^{15}/cm^2 during the initial heat treatment under vacuum. Data points for the amorphous substrate are given by ● and data points for the crystalline substrate are given by ×.

forming during metal deposition on the crystal is provided by a comparison of the thermal stability of the Pt layers on these two substrates. In Fig. 1b, the Pt(238-eV)/O(503-eV) peak ratios for both substrates have been plotted as a function of temperature for a coverage of 2×10^{15} Pt atoms/cm^2. On both surfaces, metal was deposited at 300 K and Auger spectra were taken at different temperatures during the first thermal treatment. For Pt on α-Al_2O_3{0001}, there were no significant changes in the AES peak heights, even when the sample was heated to 900 K. For Pt on the amorphous substrate, the Pt(238-eV)/O(503-eV) ratio decreased, rapidly and irreversibly, when the temperature was raised above 650 K. Increasing the temperature above 650 K had no further affect on the Auger spectrum. We attribute the changes in peak heights on the amorphous sample to aggregation of films into 3-D particles (*11*). Aggregation into particles decreases the fraction of the surface which is covered by Pt, thus decreasing the Pt(238-eV) peak and increasing the substrate O(503-eV) for a given Pt exposure. Apparently, the metal atoms on the amorphous substrate do not have sufficient mobility to form particles below 650 K. On α-Al_2O_3{0001}, 3-D particles have already formed at 300 K during metal deposition. While the formation of particles appears to be the stable configuration for both substrates, the growth of particles occurs more easily on the sapphire crystal. The reasons for the increased mobility on the crystalline sample may be due to chemical or structural effects, although it is impossible for us to differentiate these from our experiments. The α-Al_2O_3{0001} surface consists of a close-packed oxygen layer which is atomically smooth, while the amorphous alumina is probably rough and may well contain hydroxyl groups from residual water in the system. Others have also found differences in the shapes of deposited metal particles as a function of the phase and orientation of the alumina substrate (*18*).

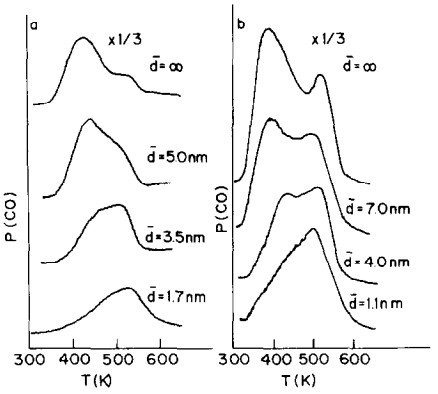

FIG. 2. (a) TPD of CO at saturation coverage from Pt particles supported on α-Al_2O_3{0001}. The heating rate for these experiments was approximately 7 K/sec. Metal exposures were 20×10^{15}, 2.0×10^{15}, 1.0×10^{15}, and 0.37×10^{15}/cm^2, respectively. (b) TPD of CO from Pt particles supported on amorphous alumina. The heating rate was maintained at approximately 10 K/sec. Metal exposures were 7.0×10^{15}, 2.0×10^{15}, 1.0×10^{15}, and 0.25×10^{15}/cm^2, respectively.

All TPD curves reported in this paper were performed on samples which had been heated to above 650 K in order to form metal particles. The average size of the Pt particles was estimated from the surface area of the metal and from the amount of metal deposited, assuming spherical particles. The metal surface areas were measured by comparing the area under the TPD curve for a saturation coverage of CO at a given metal loading to the area under the TPD curve for a continuous Pt film. While the adsorption stoichiometry for CO on Pt is known to vary by as much as a factor of 2 with particle size (*19*), we did not include correction factors since the accuracy of our measurements does not justify this precision. In any case, this will not affect the trends we have observed.

TPD of CO

Figure 2 shows the TPD results for a saturation coverage of CO from Pt particles as a function of particle size on both the crystalline and the amorphous substrates. Desorption was completely reversible for all particle sizes, and we found no evidence for

the dissociation found on small Ni and Pd particles (*20–22*). For a given particle size, the TPD curves for CO were essentially independent of the alumina substrate used. For the smallest particles, a single desorption event was observed at 510 K which has previously been assigned to desorption from metal sites with a low coordination to the surface (*11, 23*). This assignment is based on the fact that CO desorbs at this temperature on highly stepped surfaces, like Pt(331) (*12*), and on Pt(111) surfaces with defects (*14*). For larger particles, a second state centered at approximately 400 K was also observed. This state has previously been assigned to desorption from (111)-type terraces since desorption of CO from Pt(111) occurs at this temperature. The relative amounts of CO desorbing from each state varied continuously with particle size. For the α-Al_2O_3{0001} support, the fraction of CO desorbing from each state was obtained by fitting the TPD curves to two Gaussians, with the results listed in Table 1.

When TPD curves were measured as a function of CO exposure, we found that the high-temperature peak filled completely before any desorption was observed in the low-temperature peak. This sequential filling of states implies that both desorption features must be present on a given particle. Also, an exposure of 7.5×10^{14} molecules/cm^2 was sufficient to saturate the surface, indicating that the sticking coefficient for CO on the small particles was similar to that found on bulk metals (*14*).

TABLE 1

Fraction of CO Desorbing from the 400 K Peak for Pt Particles on α-Al_2O_3{0001}

Metal exposure $N(\times 10^{15}$ atoms/cm$^2)$	Particle diameter from CO adsorption (nm)	Fraction of CO in 400 K TPD peak
20.	Bulk	0.79
2.0	5.0	0.63
1.0	3.5	0.39
0.37	1.7	0.12

Assuming that the geometric interpretation for the two desorption states is correct, the fact that the TPD results from both types of alumina are very similar suggests that the final shape of the metal particles after high-temperature treatment is not strongly dependent on the oxide structure. Only the temperature required to reach the final particle shape was affected by the use of crystalline or amorphous alumina. This would imply that effects due to the interaction between the metal and the oxide are much weaker than effects due to particle size. Recent microscopy studies by Datye and co-workers also imply that some oxides may interact only very weakly with a supported metal (*24*). However, since the desorption feature at 510 K is observed on any Pt crystal which has atoms with a low surface coordination, one must be cautious not to imply too much about particle shapes from desorption features (*15*).

TPD of H_2 from Pt on Amorphous Al_2O_3

The saturation TPD curves for H_2 adsorption at 90 K on Pt particles of different sizes are shown in Fig. 3. For the continuous Pt film, H_2 desorbs in three peaks at 200, 280, and 370 K; and these three features are found to fill sequentially with H_2 exposure. Desorption features at these same temperatures are also observed on Pt crystals and foils, showing that adsorption on the small particles is qualitatively similar to adsorption on bulk metals (*5, 25, 26*). For desorption from Pt particles with diameters of 1.1 and 7.0 nm, the desorption features are less well resolved. The TPD curves show a broad peak centered at 220 K which may contain contributions from states at 200 and 280 K. The peak at 370 K decreases as the particle size decreases.

While desorption of H_2 from single crystals of Pt is complex, the variations with the crystallographic orientation are as strong as those for CO. On Pt(111), the desorption

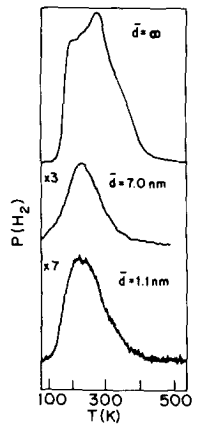

FIG. 3. TPD of H_2 from Pt particles on amorphous alumina. The heating rate was approximately 10 K/sec. Metal exposures were 7.0×10^{15}, 2.0×10^{15}, and $0.25 \times 10^{15}/cm^2$, respectively.

curve is similar to that shown for the continuous film; however, when defects are added to the surface, the desorption feature at 370 K becomes much more intense (*25*). This feature at 370 K is also very prominent for desorption from stepped crystals and polycrystalline foils (*5, 26*). Assuming that the peak at 370 K is due to sites with a low coordination to the surface, we expected to see an increase relative to the peaks at 200 and 280 K for very small Pt particles; however, the opposite appears to be true. The reasons for hydrogen desorption not following the same trends as those found for CO may be related to fundamental differences in the reasons for the multiple desorption features. Certainly, desorption of H_2 must involve two sites since H_2 adsorbs dissociatively. Also, vibrational spectra (*27*) and work function measurements (*25, 27*) for H_2 on Pt(111) imply that all the hydrogen atoms are bonded equivalently, suggesting that repulsive interactions between neighboring adsorbates, not sites of different geometry, may be primarily responsible for the different desorption states in TPD. Since the absence of the 370 K peak is observed for particles as large as 7.0 nm, it is unlikely that electronic effects could be responsible (*28–30*).

Although we cannot give a definitive reason for the H_2 TPD results, the results suggest that the conclusions reached for CO should not be interpreted as indicating the presence of bulk crystal planes. It is likely that the local site geometry plays a more important role with CO. For CO, terminal-bonded and bridge-bonded species are observed in the vibrational spectra on Pt crystals (*12*). This may imply that very small patches of metal atoms in a given symmetry are responsible for the observed features.

It should be noted that standard chemisorption experiments for H_2 on Pt/Al_2O_3 catalysts usually obtain a coverage of approximately 1.0 H/Pt_S at room temperature, while our results indicate that most H_2 desorbs below 300 K (*19*). These facts are not inconsistent. Calculations for TPD from porous materials have shown that desorption peak temperatures can easily be raised by hundreds of degrees for typical conditions, even when TPD is carried out under high-vacuum (*9*). In effect, coupling between readsorption and diffusion decreases the observed desorption rate by several orders of magnitude on porous catalysts. Support for the fact that our samples are similar to actual catalysts comes from the relative adsorption stoichiometries. Freel reported that the $H : Pt_S$ remained 1.0, independent of particle size, but that the $CO : Pt_S$ ratio changes from between 0.83 and 0.96 for small particles to 0.5 for particles larger than roughly 6.0 nm (*19*). These results imply that the ratio of the areas under the TPD curves for CO and H_2 should change by a factor of approximately 0.55 in going from small particles to the continuous film. Our actual results showed that this ratio changed by a factor of between 0.53 and 0.61. Therefore, the adsorption stoichiometries on our samples agreed very well with those obtained on actual catalysts. There is no reason to believe that desorption from actual supported catalysts should be different from that observed on our samples.

REFERENCES

1. Kelley, R. D., and Goodman, D. W., *Surf. Sci.* **123,** 743 (1982).
2. Goodman, D. W., *Surf. Sci.* **123,** 679 (1982).
3. Engstrom, J. R., Goodman, D. W., and Weinberg, W. H., *J. Vac. Sci. Technol. A* **5,** 825 (1987).
4. McCabe, R. W., and Schmidt, L. D., *Surf. Sci.* **66,** 101 (1977).
5. Collins, D. M., and Spicer, W. E., *Surf. Sci.* **69,** 85 (1977).
6. Ko, C. S., and Gorte, R. J., *Surf. Sci.* **161,** 597 (1985), and references therein.
7. Herz, R. K., Kiela, J. B., and Marin, S. P., *J. Catal.* **73,** 66 (1982).
8. Reick, J. S., and Bell, A. T., *J. Catal.* **85,** 143 (1984).
9. Gorte, R. J., *J. Catal.* **75,** 164 (1982).
10. Demmin, R. A., and Gorte, R. J., *J. Catal.* **90,** 32 (1984).
11. Altman, E. I., and Gorte, R. J., *Surf. Sci.* **172,** 71 (1986).
12. McClellan, M. R., Gland, J. L., and McFeely, F. R., *Surf. Sci.* **112,** 63 (1981).
13. Fair, J., and Madix, R. J., *J. Phys. Chem.* **73,** 3480 (1980).
14. Ertl, G., Neumann, M., and Streit, K. M., *Surf. Sci.* **64,** 393 (1977).
15. McCabe, R. W., Ph.D. thesis, University of Minnesota, 1976.
16. Tokutaka, H., Nishimori, K., and Takashima, K., *Surf. Sci.* **86,** 54 (1979).
17. Brundle, C. R., *Surf. Sci.* **48,** 99 (1975).
18. Poppa, H., Lee, E. H., and Moorhead, R. D., *J. Vac. Sci. Technol.* **15,** 1100 (1978).
19. Freel, J., *J. Catal.* **25,** 149 (1972).
20. Doering, D. L., Dickinson, J. T., and Poppa, H., *J. Vac. Sci. Technol.* **18,** 460 (1981).
21. Doering, D. L., Dickinson, J. T., and Poppa, H., *J. Catal.* **73,** 91 (1982).
22. Ladas, S., Poppa, H., and Boudart, M., *Surf. Sci.* **102,** 151 (1981).
23. Doering, D. L., Poppa, H., and Dickinson, J. T., *J. Vac. Sci. Technol.* **20,** 827 (1982).
24. Datye, A. K., Logan, A. D., and Long, N. J., personal communication.
25. Christmann, K., Ertl, G., and Pignet, T., *Surf. Sci.* **54,** 365 (1976).
26. Ko, C. S., and Gorte, R. J., *J. Catal.* **90,** 32 (1984).
27. Baro, A. M., Ibach, H., and Bruchmann, H. D., *Surf. Sci.* **88,** 384 (1979).
28. Mason, M. G., Gerenser, L. G., and Lee, S. T., *Phys. Rev. Lett.* **39,** 5 (1977).
29. Takasu, Y., Unwin, R., Tesch, B., Bradshaw, A. M., and Grunze, M., *Surf. Sci.* **77,** 505 (1981).
30. Anderson, R., "Structure of Metal Catalysts," p. 267. Academic Press, New York, 1975.

E. I. ALTMAN
R. J. GORTE

Department of Chemical Engineering
University of Pennsylvania
Philadelphia, Pennsylvania 19104

Received May 26, 1987; revised September 15, 1987